MODELING AND ACCURACY OF SOUND FIELD ANALYSIS BY FINITE ELEMENT METHOD ON BUILDING ENVIRONMENTS

Toru Otsuru and Reiji Tomiku

Oita University
Oita, 870-1192, Japan

ABSTRACT

A practical way to estimate the accuracy of sound field analysis by the finite element method in building environments is presented here. The error characteristics curves of several acoustic finite elements are proposed first, then a guideline is given for the 27-node acoustic finite element, developed by the authors, to be employed in the analysis where high accuracy is required. With the issue, sound fields in a reverberation room ($179m^3$) with several absorbent conditions are analyzed by the method to be compared with the measured values, which showed fair agreement. In the process two ways of absorption modeling are compared.

INTRODUCTION

In order to create building environments of better quality, a close investigation on acoustic condition must be of great importance. In the design process of such buildings like concert halls, lecture rooms, hospitals, residences and so on, where the acoustical considerations should be foreground, the realities of the physics of sound and the properties of human hearing must be included in the main basis of the design [1]. The computational methods can provide powerful tools for the predictions of the physical phenomena in such sound fields. This paper presents a way to analyze the sound field by means of the finite element method.

BRIEF SUMMARY OF APPROACHES TO ACOUSTICAL NUMERICAL ANALYSIS

The numerical methods, which are used to analyze sound fields, can be roughly classified into:

1) Geometrical approaches
2) Wave approaches.

As was pointed out by Rindel [2], the standard two classical geometrical methods are the Image Source Method (ISM) and the Particle Tracing Method (PTM). There is also their hybridized one, namely the Hybrid Method.

Although the ISM can provide exact results in case a room's shape is closed cavity, that is, in case no diffracted wave coming around edges exists, the relation between the number of images being taken into account and its resulting accuracy is not clear enough. Likewise, although PTM is simple and easy to be applied on actual simulations, its theoretical background is not yet clarified well.

On the other hand, finite element method (FEM), finite differential method (FDM) and boundary element method (BEM) are typical numerical methods based on the wave theory, and recently they have come to be intensively used with the progress of digital computers. Note that the former two methods divide a room's cavity into discretized nodal potentials, and the values of the potentials are derived by solving matrix equations. While, the last method requires discretization only on the room's boundary.

Generally speaking, basic characteristics of these methods are as follows: the major advantage of FDM is simplicity, but it is not easy to deal with potentials on meshes with irregular shapes by the method. On the other hand, the other two methods are easy to be applied onto the analysis of systems with complex shapes. Considering about the computer implementation, BEM is usually advantageous because less degree of freedom is required and the mesh of elements is easier to be generated in comparison with the other two. Moreover, for infinite-domain problems, since so-called Sommerfield radiation is automatically fulfilled, BEM can usually provide a simpler solution.

Nonetheless, among the numerical approaches of sound field analysis in architectural environments, or sound field in closed cavities, the finite element method is advantageous in its broad range of adaptability. Complex conditions, *e.g.* absorbent materials or temperature distribution, are easy to be involved in the FEM analysis. Although it may require more degree of freedom compared to BEM,

the symmetric sparse matrices make the computation simpler, and they are suitable to be operated in vector and/or parallel processors of up-to-date.

It is well known, however, that in the analysis based on FEM the resulting accuracy depends strongly on the interpolation function that consists the element used. While, the detailed mechanism of the approximation of sound field in the architectural environment has not been clarified yet because of the complexity of the system. Likewise, despite of its importance not enough information has provided yet to model the absorbent materials in rooms properly. In this respect, here, this paper focuses on the following two subjects; one is the accuracy of acoustic finite elements with various kinds of interpolation functions; and another is the modeling of absorbent wall conditions.

THEORETICAL DESCRIPTION

(1) Basic Formulae

The discrete formula of the sound field with sound absorption can be obtained as follows: using the ad joint system which works to describe dissipation, then kinetic, potential, and dissipated energies can be expressed in the following equations:

$$T_e = \frac{1}{4\rho_a\omega^2}\times \iiint_e (\text{grad}\, p\cdot\text{grad}\,\bar{p}^* + \text{grad}\,\bar{p}^*\cdot\text{grad}\,\bar{p}^*)dxdydz \quad (1)$$

$$V_e = \frac{1}{4\rho_a c_a}\iiint_e (p\bar{p}^* + \bar{p}p^*)dxdydz \quad (2)$$

$$J_e = \frac{i}{4\rho_a c_a\omega}\iint_e (\frac{1}{z_n}p\bar{p}^* - \frac{1}{z_n}\bar{p}p^*)dxdy \quad (3)$$

Here, z_n in equation (3) denotes the normal acoustic impedance ratio at the wall's surface. And, the work done by external force can be written in the form of

$$W_e = \frac{1}{4}\iint_{e''}(u_0\bar{p}^* + \bar{u}_0 p^* + u_0{}^*\bar{p} + \bar{u}_0{}^* p)dxdy \quad (4)$$

Then, the Lagrangian of this system can be

$$L = V - T - W + J \quad (5)$$

According to the ordinary finite elemental procedure, sound pressure at an arbitrary point in an element "e" can be approximated to be

$$p = \{N\}\{p\}_e \quad (6)$$

With this shape function, $\{N\}$, element matrices are defined as follows.

$$[K_a]_e = \iiint_e \begin{bmatrix} \frac{\partial\{N\}^T}{\partial x} & \frac{\partial\{N\}^T}{\partial y} & \frac{\partial\{N\}^T}{\partial z} \end{bmatrix} \begin{bmatrix} \frac{\partial\{N\}}{\partial x} \\ \frac{\partial\{N\}}{\partial y} \\ \frac{\partial\{N\}}{\partial z} \end{bmatrix} dxdydz$$

$$[M_a]_e = \frac{1}{c_a^2}\iiint_e \{N\}^T\{N\}dxdydz \quad (7)$$

Assuming the locally reactiveness at the wall's surface, the dissipating matrix can be obtained by

$$[C]_{e''} = \frac{1}{c_a}\iint_{e''}\frac{1}{z_n}\{N\}^T\{N\}dxdy \quad (8)$$

Substituting these matrices into equation (5), and applying Hamilton's principle, the following discrete matrix equation can be derived.

$$[M]\{\ddot{p}\} + [C]\{\dot{p}\} + [K]\{p\} = \rho\omega^2 u\{W\} \quad (9)$$

Or, using velocity potential and velocity of driving force, v, equation (9) can be in the form of

$$[M]\{\ddot{\Phi}\} + [C]\{\dot{\Phi}\} + [K]\{\Phi\} = -v\{W\}. \quad (10)$$

(2) Absorbent Element

In equation (8) the dissipation is modeled using the surface impedance. The other way to denote the dissipation in the system is to use some absorbent finite elements. One that represents a rigid porous material was given by Craggs[3] using the generalized Rayleigh model;

$$[M_{ab}]_e = \varepsilon K_s\Omega[M_a]_e$$
$$[K_{ab}]_e = \varepsilon[K_a]_e$$
$$[C_{ab}]_e = \varepsilon\frac{R\Omega}{\rho_a}[M_a]_e$$

here, $$\varepsilon = \frac{i\omega\rho_a}{R + i\omega\rho_{ab}}. \quad (11)$$

Combining these elements into equation (9) and solving it with such kernels as the linear acceleration method in the time domain, or as the modified Choleski method in the frequency domain, the acoustic response in a room with absorption can be obtained[4][5].

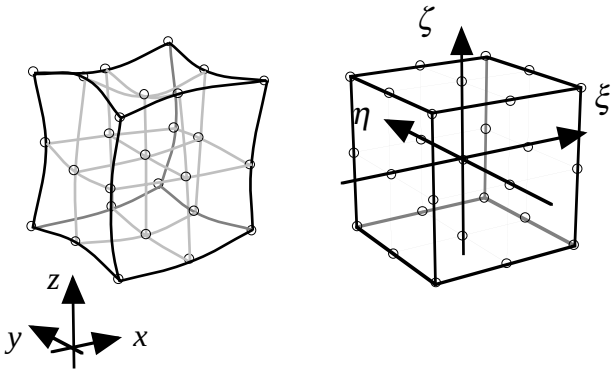

Fig.1 27-Node acoustic element (a) in global co-ordinate of (x, y, z), and (b) in local co-ordinate of (ξ, η, ζ).

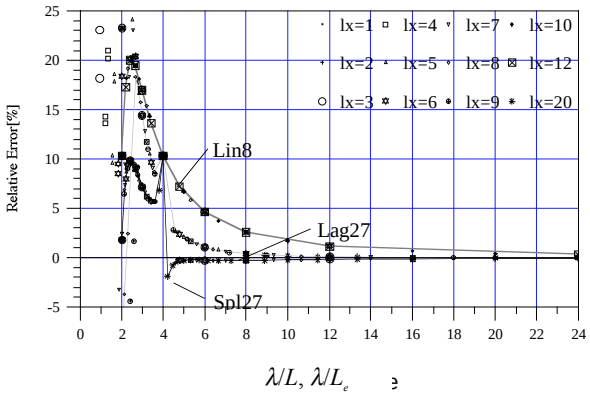

Fig.2 Error characteristics curves of eigenvalue approximation by Lin8, Lag27 and Spl27. Symbols represent the difference of numbers of spatial division (lx).

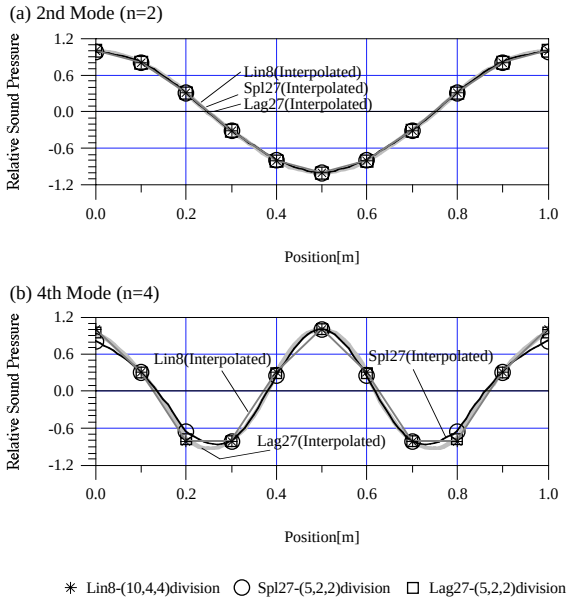

Fig.3 Approximation of eigenmode in "$\lambda./L_e$ > 4" by Lin8, Lag27 and Spl27. ((a) n = 2, $\lambda./L_e$ = 10, (b) n=4, $\lambda./L_e$ = 5)

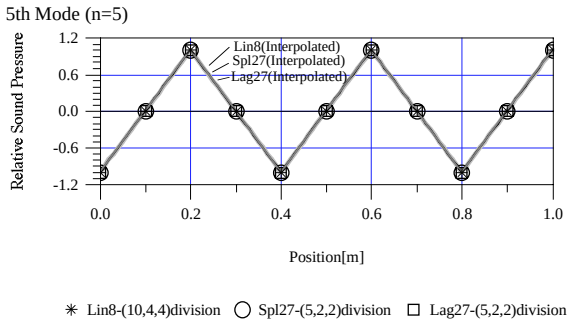

Fig.4 Approximation of eigenmode at "$\lambda./L_e$ = 4" by Lin8, Lag27 and Spl27. (n = 5, $\lambda./L_e$ = 4)

BASIC ACCURACIES OF ACOUSTIC FINITE ELEMENTS

In order to find the basic mechanism that causes the approximation errors in eigenanalysis on sound fields in rooms, an eigenanalysis on a one-dimensional sound field, a tube, with the length of 1[m] was carried out. The elements applied were Lin8, Lag27 and Spl27. Here, Lin8 is the 8- node hexahedron acoustic finite element with linear interpolation function[6], while Lag27 and Spl27 are the 27-node hexahedron elements with Lagrange and Spline interpolation functions respectively (Fig.1).

The arrays of element divisions applied here were chosen to examine only the characteristics in the tube's longitudinal direction. Fig.2 shows the error characteristics curves of eigenvalue approximation by the three elements. Regardless of elemental divisions, clear relation can be seen between the error, ε, and the ratio of λ/L; here, λ and L denote acoustic wave length and element length respectively. In the same manner, the characteristics of Spl27 and Lag27 are given there, where the L_e means lengths of half elements for these two elements. That is, the same L and L_e give the same numbers of nodal points. From Fig.2, each types of element show clear relations between the relative error in eigenvalue approximation and the ratio of λ/L (or λ/L_e). The relation characteristics do not change even if the numbers of spatial divisions, l, be changed. Furthermore, the followings can be found on each element.

As for Lin8, the ε is less than or equal to 20% throughout the region $\lambda/L \geq 2$. The ε gradually decreases as λ/L increases in the region $\lambda/L > 2.5$. On the other hand, as for Spl27, the $|\varepsilon|$ is less and about 2% in the region $\lambda/L_e > 4$; and at λ/L_e =4, the ε becomes about 10%. It is remarkable that small and stable errors within 1% can be seen throughout the

region $\lambda/L_e > 4.4$. Note that intermediate characteristics between these two elements can be seen on Lag27.

From the viewpoint of the approximation of mode shapes, several mode shapes obtained through the eigenanalysis are given in Fig.3. Each symbols denotes discrete nodal value $\{\phi_n\}$ of the modes $n = 2$ and 4, and interpolated mode shapes are also given there as each lines. Not much difference can be seen among the element types.

In the same manner, mode shapes for the n=5 are given in Fig.4. All the values obtained by the three element types locate on a straight line, which results the same interpolated sawtooth waves. It is the reason that when $\lambda/L_e = 4$, the relative errors in eigenvalue computation of the three element types become the same value, *i.e.* 10%, as is shown in Fig.2.

Thus, on the condition that $\lambda/L_e > 4$, successful interpolation of peaks in mode shapes assures the small errors in the eigenvalue approximation. The errors can be estimated using Fig.2, and for 27-node elements the half of l/L_e gives required number of elements per an acoustic wavelength.

APPLICATIONS

(1) One Dimensional Sound Field

To testify the issue given in the previous section, sound pressure computation in a one-dimensional sound field, 1.5 x 0.1 x 0.1 [m^3], was carried out using the Linear Acceleration Method to solve the equation (9) in the time domain[3]. The wall conditions were assumed to be hard and the sound source to be a tone burst with the center frequency of 500 Hz and with 6-waves. The frequency range of the tone burst lies roughly from 350 to 650 Hz.

For the Spl27 being applied to the sound field of 650Hz, a simple mathematics results that the array of element division- (5, 1, 1) gives $\lambda/L_e = 3.5$, and that the array of element division- (6, 1, 1) gives $\lambda/L_e = 4.2$. Hence, high accuracy can be expected for an analysis with the latter array because λ/L_e is larger than 4, while cannot with the former case.

With these preconsiderations, the results of the computations are shown in Figs 5 and 6 comparing

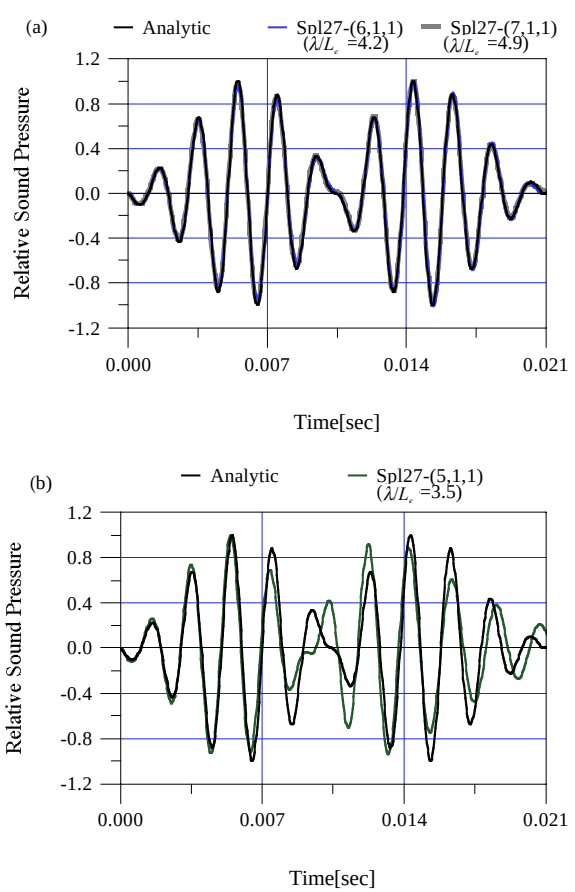

Fig.5 Comparison of sound pressure response;
(a) Analytic solution vs FEM with Spl27 (5, 1, 1)-division,
(b) Analytic solution vs FEM with Spl27 (6, 1, 1)- and (7, 1, 1)- divisions.

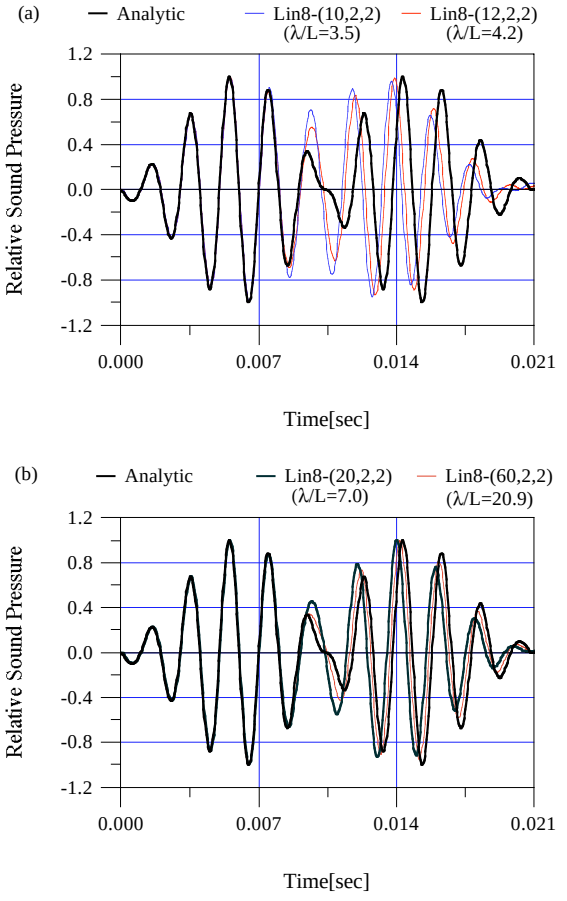

Fig.6 Comparison of sound pressure response;
(a) Analytic solution vs FEM with Lin8 (10, 2, 2)- and (12, 2, 2)- divisions, (b) Analytic solution vs FEM with Lin8 (20, 2, 2)- and (60, 2, 2)- divisions.

the difference between the arrays of element division. At first, Fig.5 shows that the Spl27 gives fair agreement if the array of element division is (6, 1, 1). Only a small change can be found if the array is increased to (7, 1, 1), or $\lambda/L_e = 4.4 > 4$, while the agreement becomes worse if the array is reduced to (5, 1, 1). These results just correspond to the preconsideration described above. To the contrary, as for the results of Lin8 in Fig.6, only small and gradual refinements are observed even if the array is increased from (10, 2, 2), or $\lambda/L = 3.5$, to (60, 2, 2), $\lambda/L = 20.9$. The degrees of freedom for the computation with the array of element division- (10, 2, 2) by Lin8 are the same as those of division- (5, 1, 1) by Spl27.

With these results, it can be summarized up that Spl27 gives excellent accuracy if $\lambda/L_e > 4$, but it is sensitive to the insufficient element division. On the other hand, Lin8 is not so sensitive against the element division but requires a finer division if higher accuracy is required.

(2) Three Dimensional Sound Field

Generally speaking, the sound fields in actual buildings have complicated boundary conditions with absorbent and/or reflective walls and floors. In this section, for the purpose of providing a basis of further applications, the sound field in a reverberation room with nonparallel walls, floor and ceiling is analyzed by FEM using Spl27 to be compared with a measurement, which verifies the accuracy of the FEM analysis with the issue given in the previous section.

(2)-1 General Settings

The room's geometry is given in Fig.7, and the measurement configuration is illustrated in Fig.8. Three conditions (C-0, C-1 and C-2) of absorbent conditions were chosen as follows:

C-0: no absorbent materials inside,
C-1: glasswool(32kg/m^3) put on one of the walls,
C-2: glasswool(32kg/m^3) put at the middle of the floor.

The main target frequency range of the investigation was set to be one third octave band with the center frequency of 200Hz, and several investigations in one twelfth octave band were carried out in case of need.

(2)-2 Configuration of FEM

In the FEM-computation, the authors employed both surface-impedance model(z_s) and absorbent-finite-element model(e_{ab}) to be compared each other, and the former is based on the equation (8), while the latter is based on the equation (11). The impedance values of the materials were given by the measurements using the transfer-function method in an impedance tube. The material constants required in the modeling of absorbent finite elements were obtained through the comparison of computed impedance values by means of FEM and Miki's equation based on an empirical model[7][8].

The acoustic element employed was Spl27 and the array of element division- (13, 13, 11) was chosen to satisfy its minimum λ/L_e be more than 4.83, which assures, based on the discussion in section 4, the accuracy of eigenvalue approximation within 1%.

The kernel to solve the matrix equation (9) employed was the modified Choleski method in the frequency domain, by which discrete values of transfer function, or sound pressure response, can be obtained in frequency-by-frequency basis. The discrete values were computed in the parallel machine distributed into 32 processors and they were summed up to be compared with the measured values in arbitrary frequency band.

(2)-3 Configuration of Measurement

A one-twenty-fourth octave band SPL-measurement at the center frequency of 200Hz was carried out

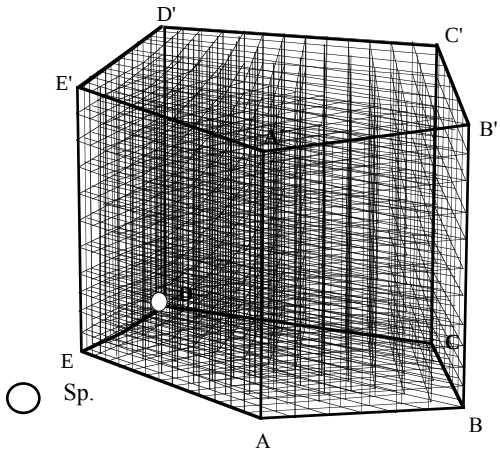

Fig.7 Geometry of reverberation room and its mesh division applied in the FEM analysis(V=179m^3).

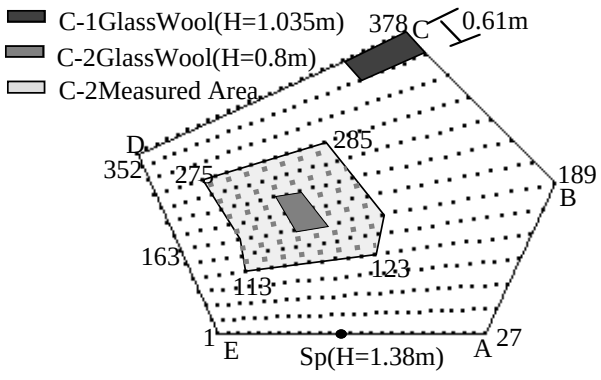

Fig.8 Configuration of measurements. Dots represent computed/measured points, in C-0 and C-1, on the cross section at 1.2 m high.

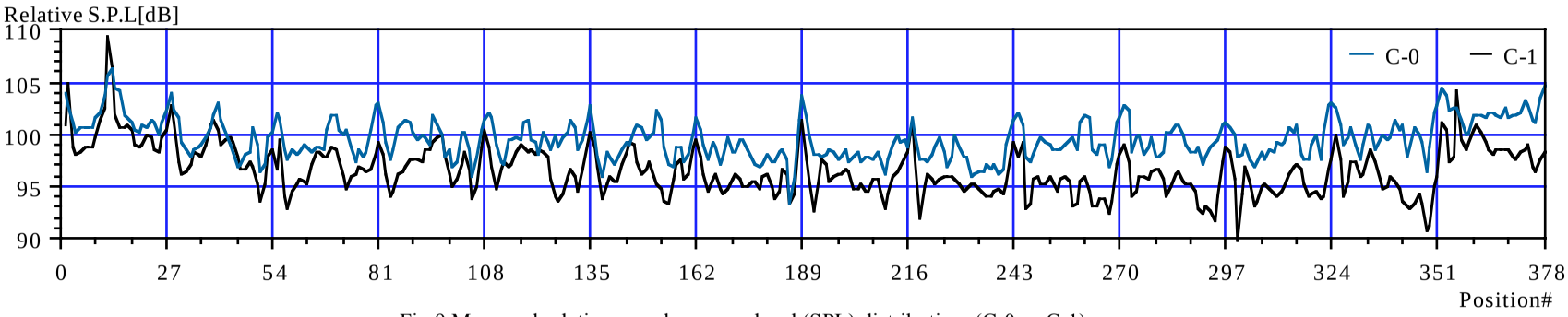

Fig.9 Measured relative sound pressure level (SPL) distribution; (C-0 vs C-1)

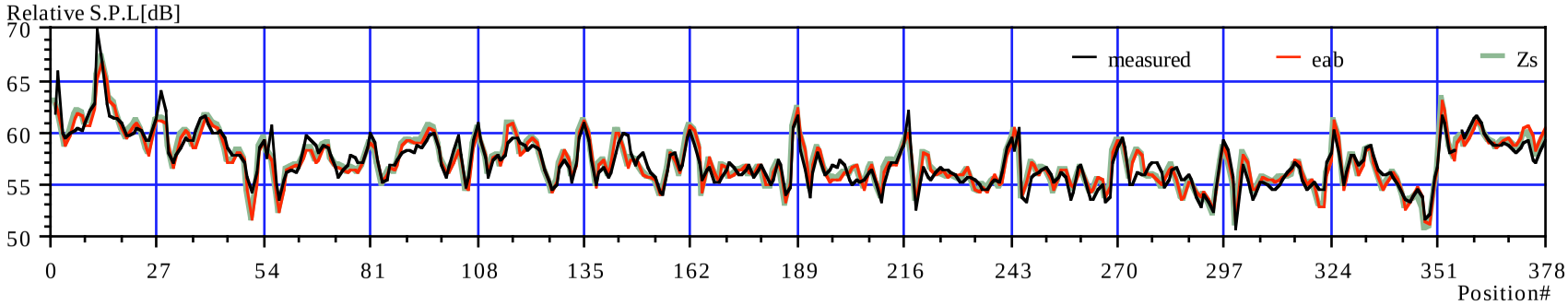

Fig.10 Comparison between FEM and measurement on C-1 in one-third octave band.

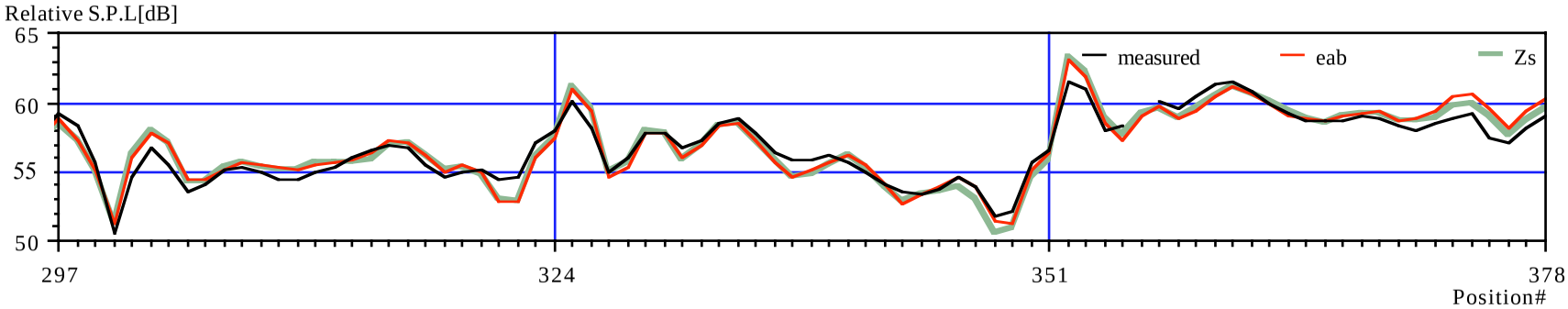

Fig.11 Detail of the SPL distribution around the glasswool at a corner of the reverberation room.(C-1)

using a two channel digital filter (B&K 2144). The SPL in one-third octave band was obtained by summing up the measured values. The numbers of measured points are 378 for both C-0 and C-1, while the number for C-2 is 1001 that cover the five surfaces of a block of glasswool as is shown in Fig.8.

(2)-4 Results and Discussion

At first, the effect of the absorption in the sound field was examined by comparing the measured relative sound pressure level (SPL) distributions (Fig. 9). The difference of SPL between C-0 and C-1 rose up to about 5 dB, and the difference becomes larger when the receiving point is closer to the absorbent material.

Second, a comparison between FEM and measurement on C-1 in one-third-octave band is given in Fig. 10, and Fig.11 shows the detail of the SPL distribution near the glasswool at one of the corners of the reverberation room. In the figures, there also compared is the difference of absorbent modeling, e_{ab} and z_s. Fair agreement of FEM and measurement can be seen at and around the peaks and dips of SPL distribution in the sound field. As for the absorbent modeling, only a slight difference can be found in this case. Generally speaking, FEM can give the detailed information of the potential distribution in the system, so the three dimensional transfer function distributions in sound fields in buildings can be given by the method; and Fig.12 is an example of them, which shows two-dimensional distribution of SPL in the room; and, in addition, the SPL values of FEM were obtained from the values of computed transfer functions.

Finally, the difference of absorption modeling was investigated. In the case of C-2, where the transmitted sound through absorbent porous material exists, the difference between the models can be expected to be larger because the modeling- z_s takes into account only of locally reactiveness, while modeling- e_{ab} can represent extended reactiveness. The comparison is given in Figs 13 (on the cross section at 0.6m high) & 14 (at 0.8m high), in which plotted are SPL values at the143 points around the block of glasswool; and these points on the cross sections are picked up from the measured 1001 points originally. The FEM results with modeling- z_s shows some difference from the other two around the block of glasswool, while FEM results with modeling- e_{ab} generally agrees with measured values including the points from 44 to 55 in the Fig.13 where the points are on the surface of the glasswool. Hence, it can be summarized up on the absorption modeling that the modeling- z_s is simpler and easier to be combined into the system, but when the assumption of locally reactiveness does not stand modeling- e_{ab} is better to be applied.

CONCLUSIONS

The FEM sound field analysis with 27-node element, Spl27, is discussed and finally its accuracy in an application onto a three dimensional sound field in a reverberation room has been confirmed experimentally. The accuracy can be established by controlling the dimensions of elements used to be $\lambda/L_e > 4$, which leads about 1% relative error in eigenvalue approximation. Example computations on both tube and reverberation room have also validated the accuracy of their sound pressure approximations. Since detailed information of the sound field, such as transfer function distributions in three dimensional fields, can be obtained by the method with distinct guideline for its resulting accuracy, further investigations on and around room acoustics in building environments become effective enough to be dealt with from the viewpoint of wave/physical acoustics.

ACKNOWLEDGEMENTS

The authors are indebted to the former graduate students K. Fujii, Y. Takahashi, A. Fujita, T. Uchida and Purnomo for the computer implementation of the concepts developed through this research and also for their cooperative works in measurements. This work was supported, in part, by the Grand-in Aid for Science Research(B) 10450214. The main part of the computation was carried out on Fujitsu VPP 700/64 in the Computing Center Kyushu University, Fukuoka, Japan.

REFERENCES

[1] Marshall, A. H. and Cavanaugh, A. J., Architectural Acoustics, Encyclopedia of Acoustics, Vol. III, John Wiley & Sons, New York, 1997

[2] Rindel, J. H., Naylor, G., "Computer Modeling of Sound Fields in Rooms – The State of the Art and Outlook to the Future -," ICA 14, F2-1, 1992

[3] V. Easwaran and A. Craggs, "On Further Validation and use of the Finite Element Method to Room Acoustics," J. of Sound and Vib., 187(2), 195-212, 1995

[4]T. Otsuru, K. Fujii, "Finite elemental analysis of sound field in rooms with sound absorbing materials," Proceeding of Inter-Noise 94, 2011-2013, 1994

[5] T. Otsuru, T. Uchida, " A Discussion on Finite Elemental Analysis of Sound Field in Rooms with Sound Absorbing Materials," Fifth International Congress on Sound and Vibration AVol.2 App.809-817, 1997

[6] A. Craggs, Acoustic Modeling, "Finite Element Method, Encyclopedia of Acoustics," Chapter 14, John Wiley & Sons, New York, 1997

[7] Y. Miki, "Acoustical Properties of Porous Materials - Generalizations of empirical models -," J. Acoust. Soc. Jan.(E), pp.25-30, 11, 1, 1990

[8] R. Tomiku, T. Otsuru, " Finite elemental analysis of sound field in rooms -Basic investigation of modeling of absorbent materials-," AIJ Kyushu Chapter Architectural

Research Meeting (Environment), No.38.2, pp.69-72, 1999 (in Japanese)

NOMENCLATURE

c_a : Velocity of sound,
i : Square root of (-1),
K_s : Structure constant,
R : Flow resistance,
z_0 : Specific acoustic impedance of air,
r_a : Air mass, ($z_0 = \rho_a c_a$),
ρ_{ab} : Material density,
λ : Acoustic wavelength,
Ω : Porosity,
ω : Angular frequency,
$[M],[K],[C]$: Mass, stiffness, and damping matrices,
$\{N\}$:Shape function,
$\{W\}$: Distribution vector,
$\{p\}$: Nodal sound pressure vector,
$\{\Phi\}$: Velocity potential vector,
$\dot{p}$: dp/dt,
z^* : Complex conjugate of the complex number z,
$[\ ]^T, \{\ \}^T$: Transpose of [ ], { }.

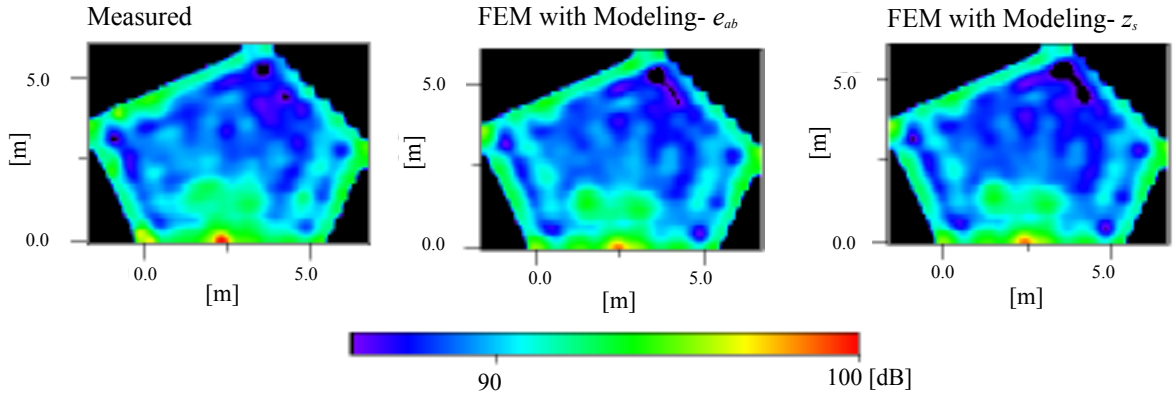

Fig.12 Contour map of SPL distribution in the reverberation room. (C-1)

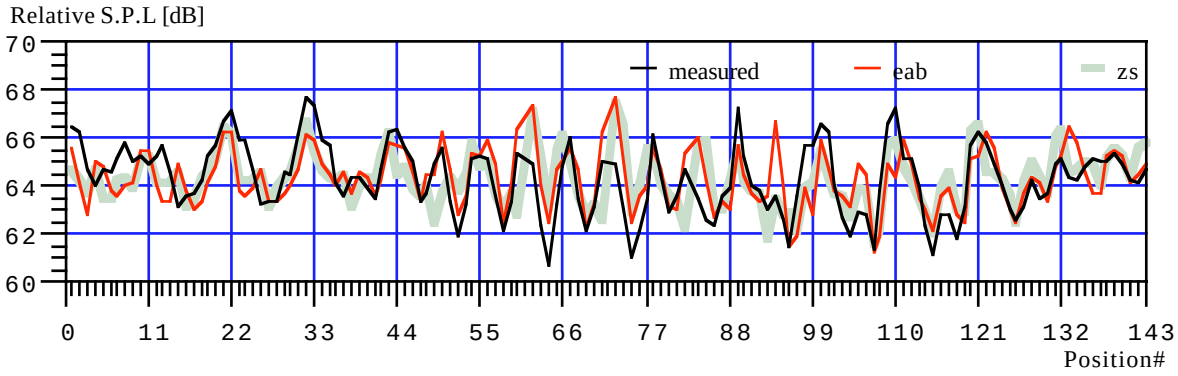

Figs 13 Comparison of absorption modelings, z_s vs e_{ab}. (on the cross section at 0.6m high, C-2)

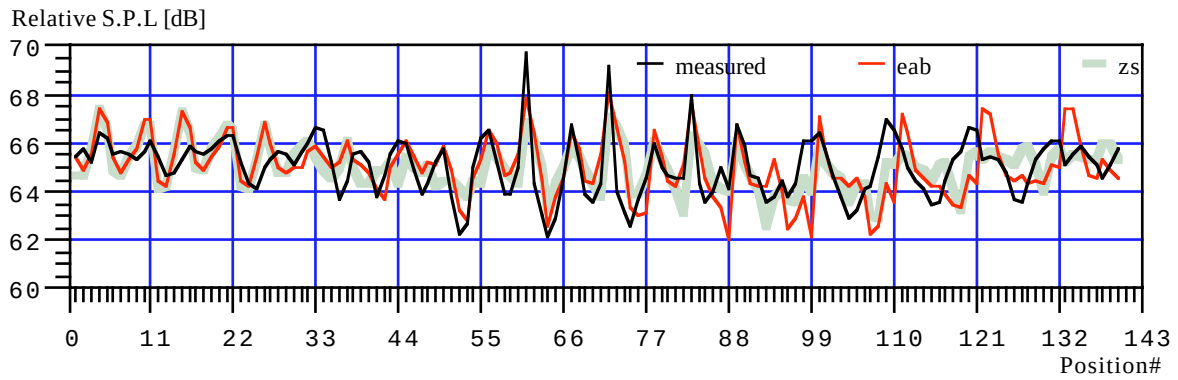

Figs 14 Comparison of absorption modelings, z_s vs e_{ab}. (on the cross section at 0.8m high, C-2)